Biochemical and Biophysical Research Communications 437 (2013) 489–495

Contents lists available at SciVerse ScienceDirect

Biochemical and Biophysical Research Communications

journal homepage: www.elsevier.com/locate/ybbrc

Matrix-specified differentiation of human decidua parietalis placental stem cells

Indumathi Sridharan [a], Taeyoung Kim [a], Zuzana Strakova [b], Rong Wang [a,*]

[a] Department of Biological and Chemical Sciences, Illinois Institute of Technology, 3101 S. Dearborn St, Chicago, IL 60616, United States
[b] Department of Obstetrics and Gynecology, 820 S. Wood Street, M/C 808, Chicago, IL 60612, United States

ARTICLE INFO

Article history:
Received 27 June 2013
Available online 10 July 2013

Keywords:
Collagen
Carbon nanotubes
Stem cells
Neural differentiation

ABSTRACT

To create suitable biological scaffolds for tissue engineering and cell therapeutics, it is essential to understand the matrix-mediated specification of stem cell differentiation. To this end, we studied the effect of collagen type I on stem cell lineage specification. We altered the properties of collagen type I by incorporating carbon nanotubes (CNT). The collagen–CNT composite material was stiffer with thicker fibers and longer D-period. Human decidua parietalis stem cells (hdpPSC) were found to differentiate exclusively and rapidly towards neural cells on the collagen–CNT matrix. We attribute this accelerated neural differentiation to the enhanced structural and mechanical properties of collagen–CNT material. Strikingly, the collagen–CNT matrix, unlike collagen, imposes the neural fate by an alternate mechanism that may be independent of beta-1 integrin and beta-catenin. The study demonstrates the sensitivity of stem cells to subtle changes in the matrix and the utilization of a novel biocomposite material for efficient and directed differentiation of stem cells.

1. Introduction

Lineage-specific differentiations of stem cells are resulted from the concerted efforts of physical and chemical cues within the niche [1]. Derivation of neural progenitors and functional neural cells from stem cells offer considerable hope of cellular replacement therapies for neuro-degenerative disorders like Alzheimer's. A significant study by Engler et al. implied that, although the presence of soluble factors augments lineage acquisition, the appropriate extracellular matrix (ECM) properties can promote the neural fate in mesenchymal stem cells [2]. Dalby et al. reported similar specifying capabilities of a nanostructured matrix on osteogenic differentiation in mesenchymal stem cells [3]. These studies implied that the physical cues and the biochemical signals transmitted by cell–matrix interactions are sufficient to promote directed differentiation [4,5].

In our previous study on neural differentiation of human embryonic stem cells [6], we found that the collagen type I – carbon nanotube (collagen–CNT) composite matrix promoted an efficient and rapid neuroectodermal commitment in a non-selective medium (that allows random and spontaneous differentiation). In this study, we investigated the matrix-directed lineage commitment of human decidua parietalis placental stem cells (hdpPSCs). hdpPSCs, previously known as human uterine fibroblasts, were first derived by Strakova et al. [7]. These adult stem cells are much more robust and easily derived and hence, are preferable for *in vitro* studies and clinical therapies. Here we report on the early neural marker expression profile on gelatin, collagen and collagen–CNT matrices under the spontaneous differentiation condition. We reaffirm the neural commitment and maturation of the hdpPSCs are accelerated on collagen–CNT matrix. In addition, we identify putative neural commitment mechanisms on collagen and collagen–CNT matrices based on the distinct role of beta-1 integrin.

2. Materials and methods

2.1. Matrix preparation and cell culture

A variety of matrices were prepared according to our previously published method [6]. In the current study, 1.5 mg/ml collagen solution was utilized to prepare for the collagen matrix. Collagen–CNT solution was prepared by adding 5 μg of oxidized CNT per ml of collagen solution. 0.1% gelatin (Fisher scientific, Fairlawn, NJ) was used to prepare for the control matrix.

Undifferentiated hdpPSCs (passage 2–3) were obtained from Dr. Strakova's lab and propagated in a self-renewal media according to their pre-defined protocol [7]. For differentiation experiments, the undifferentiated cells at passage 3–5 were trypsinized and plated on various matrices in the non-selective, spontaneous differentiation medium (DMEM + 10% FBS + 1% non-essential amino acids) at a density of 5000 cells/cm^2 per matrix.

* Corresponding author.
E-mail address: wangr@iit.edu (R. Wang).

0006-291X/$ - see front matter © 2013 Elsevier Inc. All rights reserved.
http://dx.doi.org/10.1016/j.bbrc.2013.07.002

2.2. AFM measurements

A multimode Nanoscope IIIa AFM (Veeco Metrology, Santa Barbara, CA), equipped with a J-scanner, was utilized in this study. Both AFM imaging and stiffness measurements were carried out in PBS buffer using Si_3N_4 tips with a spring constant of 0.056 ± 0.002 N/m, calibrated by using reference cantilevers with known spring constants. The substrate stiffness measurements were conducted by employing an AFM tip as a nano-indenter to generate force spectra, from which the Young's modulus, *E*, was derived using the Hertzian model [8–10]. The average *E* was calculated from E-maps consisting of a minimum of 25 data points per area, and measured from at least five areas in different samples using different tips.

2.3. Immunofluorescence staining

A Nikon U-2000 microscope was used to collect the immunofluorescent images. The expression of nestin and SOX1 was tracked at 8 h, Day 1 and Day 3 post-plating. The expression of Tuj-1 and NeuN was examined in cells after a week in culture. For each experiment on a particular marker, the exposure time and gain value were kept constant throughout the entire study across all matrix samples and time points. The primary antibodies used in this study include rabbit anti-Nestin (Millipore, Billerica, MA, 1:200 dilution), rabbit anti-SOX1, (Abcam, Cambridge, MA, 1:200 dilution), rabbit anti-Beta-1 integrin (BD biosciences, San Jose, CA, 1:500 dilution), rabbit anti-Beta-3 tubulin (Tuj 1, Abcam, Cambridge, MA, 1:200 dilution) and mouse anti-NeuN (Millipore, Temecula, CA, 1:100 dilution). Secondary antibodies were purchased from Invitrogen (Carlsbad, CA) and used at a dilution of 1:200. Negative control was performed by excluding the primary antibody during the staining protocol for each matrix for every trial.

The immunofluorescent images were quantitatively analyzed by ImageJ, a software developed by NIH. Image size, magnification and imaging parameters were maintained constant throughout all measurements to avoid variations between samples. In determining the percentage of positively stained cells, a cell is considered positive when its fluorescence intensity is two folds or more above the background. For transcription factors such as SOX1, NeuN and beta-catenin, the nuclear staining was measured to determine the positively stained cells.

2.4. Beta-1 integrin blocking experiments

An antibody targeting to the N-terminal of beta-1 integrin (Abcam, Cambridge, MA), termed blocking antibody, was chosen to block the beta-1 integrin interaction with the matrices. 1 μg/ml blocking antibody was supplied to the medium at the time of cell plating, resulting in sufficient and reproducible differences compared to the control. For neural commitment studies, the expression levels of beta-1 integrin (using C-terminal specific antibody), SOX1 and beta-catenin were examined in cells at 1 and 4 h post-plating.

3. Results

3.1. Characterization of matrices and the matrix directed cell growth

As shown in the phase images in Fig. 1A–C, densely distributed fibers are visible on collagen and collagen–CNT matrices while the gelatin surface is homogeneous. In the structured matrices, a crude alignment of fibers is visible upon dip-coating. The nanoscopic surface features of the matrices were examined by AFM. As shown in Fig. 1D–F, the gelatin surface is feature-less with a surface roughness of 4.2 nm. Collagen fibers are ~50 nm in diameter with a D-period of 68 ± 1 nm. Collagen–CNT fibers are thicker (225 nm in diameter) with an extended D-period of 70 ± 1 nm. The difference in D-period is statistically significant ($p < 0.001$) according to the *t*-test. We also examined the matrix stiffness by using the nano-indentation method, and derived the mean values of Young's modulus for gelatin, collagen and collagen–CNT matrices to be 0.07, 0.123 and 0.240 MPa, respectively. The longer D-period suggests that the addition of CNT to collagen causes a molecular level alteration of the collagen fiber assembly. The formation of thicker bundles is likely the result of CNT enhanced collagen-collagen association during the assembly process. The results are consistent with our previous observations [6].

To understand the cell–matrix interaction, we examined hdpPSCs on Day 3 of differentiation in a non-selective medium. Most cells on gelatin showed irregular and polygonal shapes (Fig. 1G). On collagen and collagen–CNT matrices, however, almost all cells observed were bipolar. The cell projection on collagen–CNT (648 ± 262 μm) was much longer than that on collagen (458 ± 129 μm) (Fig. 1H, I – red arrows). Strikingly, the cells on collagen–CNT were well-aligned with respect to each other, following the crude alignment of the dip-coated matrix. On collagen, such alignment was not always present. No cell alignment was seen on gelatin matrix. These results suggest that matrix features influence the cell shape and alignment.

3.2. Neural commitment on various matrices

By Day 3 of hdpPSC differentiation in a non-selective medium, we did not find any specification towards endoderm or mesoderm in cells on any of the matrices (data not shown). However, the cells showed noticeable expression patterns of nestin and SOX1, which are markers for neuro-ectoderm (Fig. 2A). SOX1 is a transcription factor and is the earliest marker for neural commitment *in vitro* [11,12]. Down-regulation of SOX1 marks the transition from committed neural precursors to neural progenitor phenotypes [13]. ImageJ analysis suggests that by 8 h of culture, SOX1 was expressed by 60% of the population on collagen–CNT compared to 28% on collagen and only 6% on gelatin (Fig. 2B). Moreover, the SOX1 (+)ve to SOX1 (−)ve transition occurred by Day 1 in cells on collagen–CNT as indicated by the decline in the expression level and the percentage-positive data. The cells on collagen maintained the same SOX1 expression level initially and dropped by Day 3. Thus, collagen–CNT imposes early neural fate commitment and rapid transition to progenitor phenotypes. These expression patterns were reflected at the mRNA level (not shown).

The lower panel of Fig. 2A shows the nestin-positive cells observed on all matrix types. Nestin, an intermediate filament protein, is expressed highly by neural progenitors [14]. Nestin-positive proliferating cells have the potential to differentiate into neuronal or glial cells [15]. On both collagen and collagen–CNT, the cells staining nestin strongly were also bipolar in shape. On gelatin, the strongly positive cells were rarely bipolar, and were usually surrounded by cells expressing little or no nestin. From Fig. 2C, the nestin expression level and the percentage of positively stained cells continuously increased over the 3-day time period on collagen–CNT. These values were much higher than those on collagen and gelatin. Although nestin's function is not completely understood, it is involved in the organization & maintenance of elongated cellular morphology of neuro-epithelial precursors [16]. Thus, the high nestin expression on collagen–CNT may be involved in producing the highly elongated cellular morphology. Interestingly, although collagen supported SOX1 expression at a high level and in a significant cell number, the nestin expression level was lower than that on collagen–CNT and the number of nestin-positive cells increased only modestly by Day 3. Taken together, as of

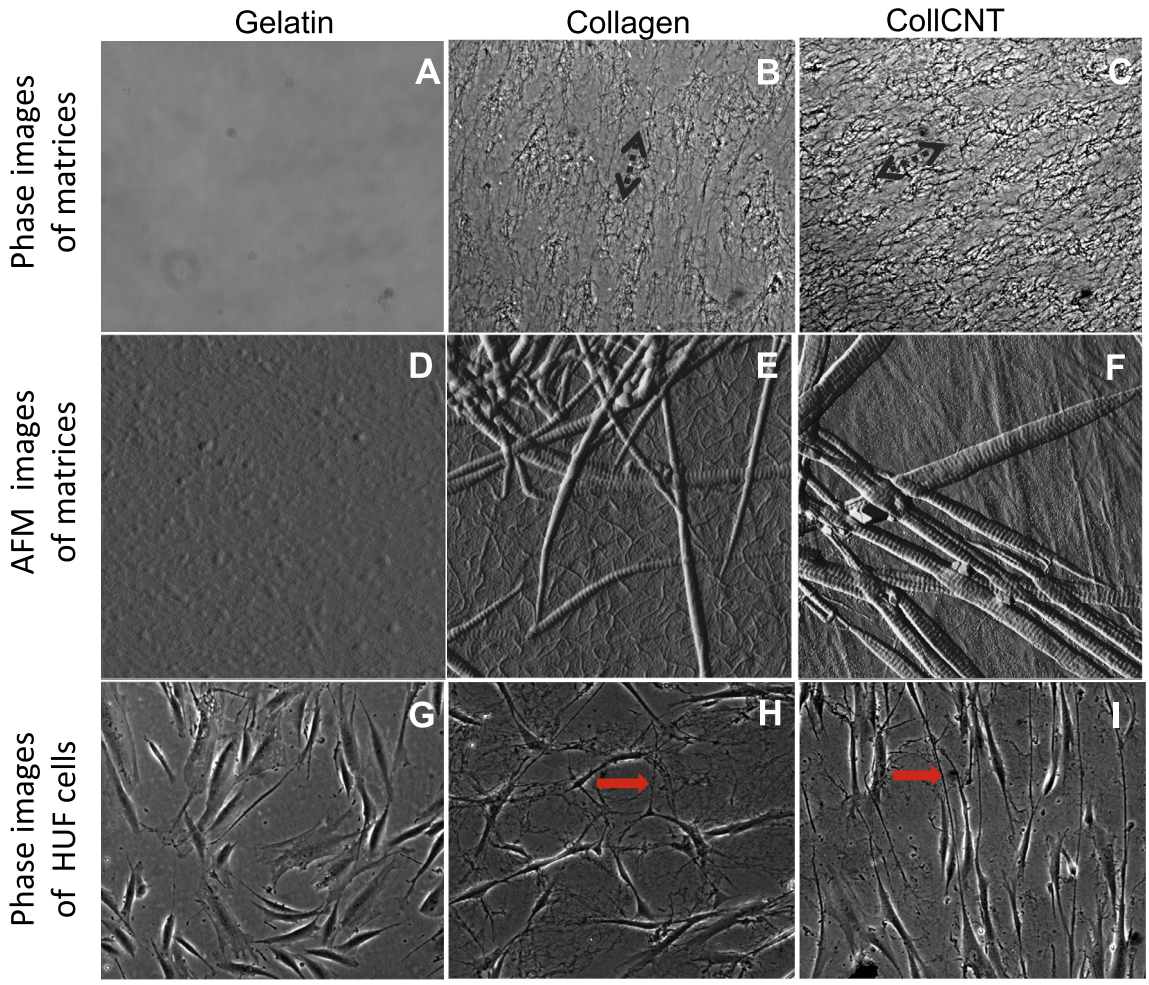

Fig. 1. Characterization of various matrices and the cell growth. (A–C) Phase images of gelatin (A), collagen (B) and collagen/CNT (collCNT) (C) matrices showing the microscopic surface features. Magnification: 10×. (D–F) 8.5 × 8.5 μm^2 AFM images (in amplitude mode) illustrating the nanoscopic surface features of the matrices. (G–I) Phase images of the hdpPSCs at Day 3 of differentiation on gelatin (G), collagen (H) and collCNT (I) matrices. The red arrows point to cell projections. Magnification: 10×. (For interpretation of the references to colour in this figure legend, the reader is referred to the web version of this article).

Day 3, it appears most cells on collagen–CNT were established neural progenitors, while cells on gelatin and collagen lagged behind.

By Day 6, we identified many cells with dendritic morphology (yellow dotted arrows) on collagen–CNT (Fig. 3). These cells were positive for either Tuj-1 or NeuN. On collagen, only Tuj-1-positive cells were predominantly observed by Day 6 and NeuN staining was barely detectable. In contrast, on gelatin, neither Tuj-1 nor NeuN staining was observed. Thus, the collagen–CNT matrix is capable of supporting the development of mature neuronal cells at a faster pace than collagen and gelatin.

3.3. Beta-1 integrin expression profile

The aforementioned study established that the matrix properties dictate the neural fate in hdpPSCs. In order to understand how collagen and collagen–CNT matrices elicit their different neural commitment/differentiation response in hdpPSCs, we focused on beta-1 integrin, the transmembrane adhesive receptor protein. As the specific cell surface receptor of collagen, beta-1 integrin is a key component to sense and transmit physical and chemical cues of the matrix to intracellular signaling pathways.

To reveal the effect of beta-1 integrin, a blocking antibody (targeting to the N-terminal domain of beta-1 integrin) was applied to cells during adhesion, and the expression level of beta-1 integrin was profiled using an antibody specific to the C-terminal (Fig. 4A). The experiments were carried out on collagen and collagen–CNT matrices at 1 and 4 h post-plating. Under the control condition while no blocking antibody was applied, cells on collagen expressed a higher level of beta-1 integrin than those on collagen–CNT (Fig. 4B, i and ii). At 1 h post-plating, the percentage of beta-1 integrin positive cells (β-int$_{\%pos}$) was also higher on collagen (13%) than on collagen–CNT (5%) (Fig. 4C). The application of blocking antibody reduced the beta-1 integrin expression level and the β-int$_{\%pos}$ on pure collagen (Fig. 4B (iii) and C). On collagen–CNT (Fig. 4B (iv) and C), on the contrary, blocking beta-1 integrin caused a significant increase in beta-1 integrin expression and an increase in the β-int$_{\%pos}$. At 4 h post-plating, we found the change of β-int$_{\%pos}$ followed the same trend as at 1 h post-plating while the β-int$_{\%pos}$ increased by 2–4-fold on both matrices under either condition. The results suggest that blocking beta-1 integrin has matrix-dependent effects on endogenous beta-1 integrin expression.

3.4. Effect of blocking beta-1 integrin on neural commitment

Beta-1 integrin is linked to nuclear accumulation of beta-catenin [17], a well-established regulator of neural differentiation. In order to test the role of integrin in neural commitment in our system, we examined the percentage positive cells for SOX1 (SOX1$_{\%pos}$) and beta-catenin (β-cat$_{\%pos}$) at 1 h post-plating under control and beta-1 integrin blocked conditions. The results are

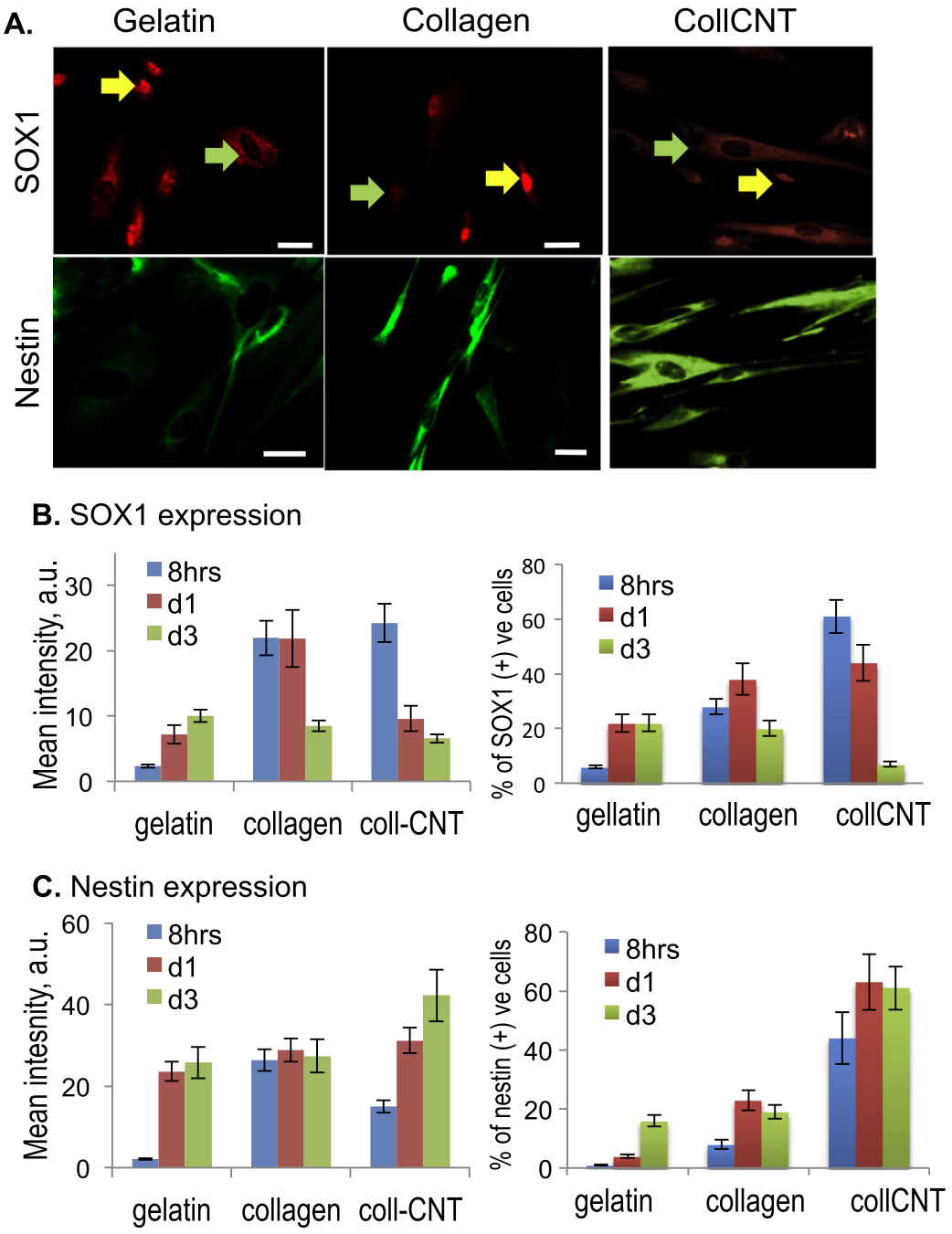

Fig. 2. Neural lineage specification in hdpPSCs. (A) Immunofluorescent images showing the SOX1 and Nestin positive cells on various matrices at Day 3 of differentiation. Bar size: 100 μm. Typical SOX1 (+) and SOX1 (−) cells are indicated by the yellow and green arrows, respectively. (B,C) ImageJ quantification of the expression levels of SOX1 (B) and Nestin (C) in cells on various matrices, illustrated in both the mean fluorescence intensity and the percentage of positively staining cells. $n = 100$. (For interpretation of the references to colour in this figure legend, the reader is referred to the web version of this article).

summarized in Fig. 4C. Unless otherwise specified, the expression pattern of the proteins followed the same trend at 4 h post-plating.

Under control conditions, lower β-cat$_{\%pos}$ was observed on collagen–CNT than on collagen, mirroring the beta-1 integrin expression pattern. On collagen, blocking-induced reduction in β-int$_{\%pos}$ is reflected in the reduced β-cat$_{\%pos}$. On collagen–CNT, blocking-induced increase in β-int$_{\%pos}$ is correlated with a greater β-cat$_{\%pos}$. Thus, it appears that beta-1 integrin is linked to beta-catenin expression in cells on both matrices. On collagen, when beta-1 integrin and beta-catenin were both highly expressed (i.e, under the control condition), high SOX1$_{\%pos}$ was observed. The reduction in beta-1 integrin and beta-catenin upon blocking coincided with the dramatic reduction in SOX1$_{\%pos}$. There appears to be a direct relation among the three proteins in cells on collagen matrix. It is conceived that, upon adhesion to the collagen matrix, the beta-1 integrin may trigger biochemical pathway of neural fate commitment (i.e, SOX1 expression) via beta-catenin.

On collagen–CNT, although the β-int$_{\%pos}$ was lower than that on collagen under the control condition, the SOX1$_{\%pos}$ was much higher (70% at 1 h post-plating). Moreover, blocking-induced up-regulation in beta-1 integrin and beta-catenin in cells on collagen–CNT significantly reduced the SOX1$_{\%pos}$ to just 6% at 1 h of post-plating, indicating an inverse correlation between beta-1 integrin (and beta-catenin) and SOX1. However, it must be noted

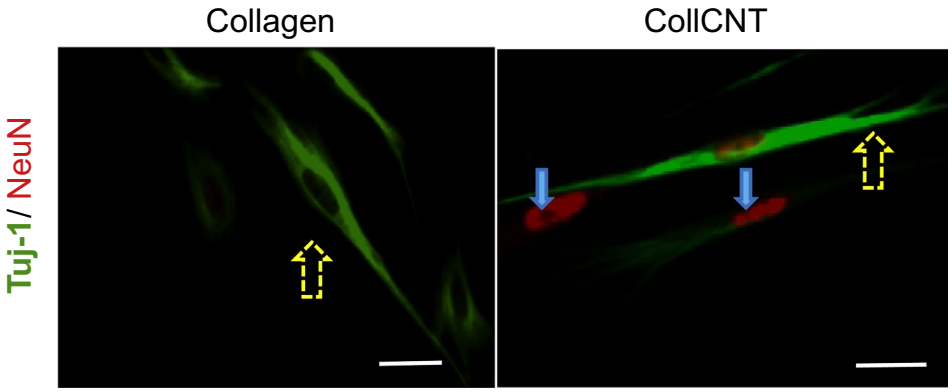

Fig. 3. Immunofluorescent images of hdpPSCs at Day 6 of differentiation on collagen and collCNT, staining against Tuj-1 (green) and NeuN (red). The yellow dotted arrows and the blue arrows indicate the Tuj-1 and NeuN strongly positive cells, respectively. Bar size: 100 μm. (For interpretation of the references to colour in this figure legend, the reader is referred to the web version of this article).

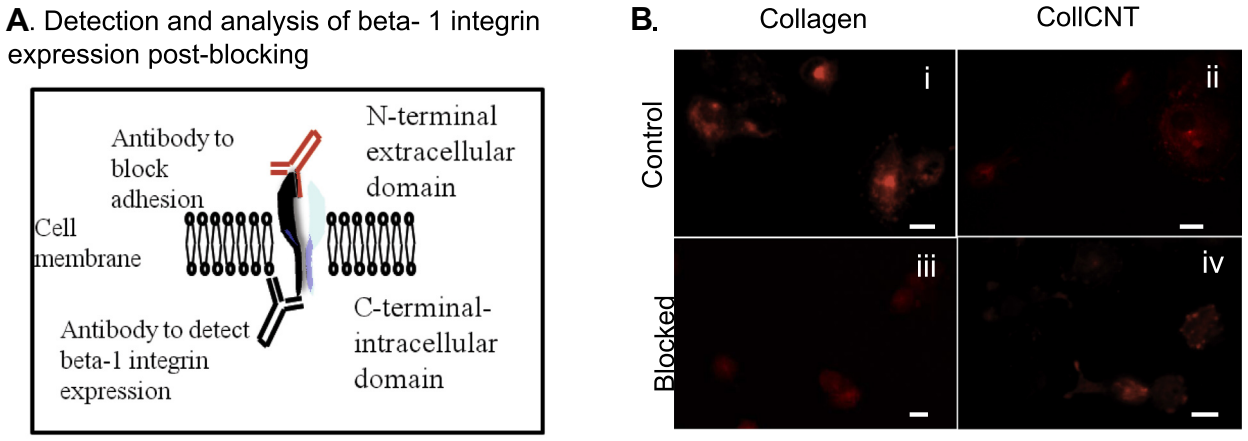

C.

	Collagen		CollCNT	
	Control	Blocked	Control	Blocked
Beta-1 integrin	13±2%	9±2%	5±1%	32±10%
Beta-catenin	88±10%	42±10%	43±9%	69±6%
SOX1	50±12%	4±1%	70±8%	6±2%

Fig. 4. Beta-1 integrin expression profile. (A) Schematic of detecting beta-1 integrin expression post-blocking. (B) Immunofluorescent images of beta-1 integrin expression in cells on collagen and collCNT at 1 h post-plating with (iii, iv) and without (i, ii) the addition of 1 μg/ml blocking antibody to the medium at the time of cell plating. Bar size: 150 μm. (C) Percentage of cells positive for beta-1 integrin, SOX1 and beta-catenin at 1 h post-plating on collagen and collCNT under control and beta-1 integrin blocked conditions. $i = 100$.

that at 4 h post-plating under the blocking condition, the $SOX1_{\%pos}$ increased to 46% on collagen–CNT, implying that the increase in beta-1 integrin expression did not completely deter but delayed the incidence of SOX1 in cells on collagen–CNT. The relative mRNA levels (not shown) at 1 and 4 h also indicated a similar trend of SOX1 expression. From these observations, we conclude that although beta-1 integrin may be linked to beta-catenin in cells on collagen–CNT, the SOX1 expression either unnecessarily requires high beta-1 integrin expression/incidence or is negatively impacted by the increase in beta-1 integrin and beta-catenin, pointing to an inverse correlation. Based on these data, we speculate that unlike on collagen, the neural commitment pathway on collagen–CNT likely does not require the high beta-catenin and/or beta-1 integrin expression.

Considering that beta-1 integrin is primarily an adhesion protein, the low expression of beta-1 integrin in cells on collagen–CNT may lead to low cell-matrix adhesion strength, indicating the role of mechanotransductive pathway. We used a trypsin de-adhesion assay [18] to deduce the adhesion strength of cells to collagen *vs.* collagen–CNT within an hour of plating under

control and beta-1 integrin blocked conditions. By monitoring the cell area decrease over time upon trypsinization, we derived the earliest saturation time point when there is no more reduction in cell area in the presence of trypsin. Combined with the data in Fig. 4C, the results indicate that on matrices where beta-1 integrin expression level was lower (or higher), the saturation time point was lower (or higher) and hence, the adhesion was reduced (or increased). Thus, the level of beta-1 integrin expression in cells on a matrix is correlated to the strength of cell adhesion. The low adhesion between the cells and the collagen–CNT matrix may trigger an alternative mechanotransductive pathway resulting in the enhanced neural commitment phenomena on collagen–CNT, as further delineated in the next section.

3.5. Discussions

The extracellular matrix proteins provide unique structural and chemical cues to regulate the stem cell differentiation. As a ubiquitous ECM structural protein, collagen is well-suited for studies on matrix-mediated effects on stem cell differentiation. The structure of collagen type I possesses well-formed fibers of specific dimension and stiffness (Fig. 1). Unlike the amorphous surface of gelatin, the fibrous structure of collagen can generate neural precursors and progenitors that proceeded towards largely Tuj-1 expressing immature neuronal cells by Day 6 (Fig. 3). The specific ligands and the appropriate stiffness of collagen may have played a role in its neural fate specifying capacity, as observed by others [9,19]. This observation suggests that the unique molecular, structural and mechanical features of the matrix protein were sufficient to specify cell fate without the need of pro-neural soluble factors. Therefore, collagen is a useful matrix for deriving neural cells.

We and others have reported that CNT is capable of promoting neural differentiation of stem cells [6,20,21]. Here, we observed that CNT augmented the capabilities of collagen as a matrix for neural differentiation of hdpPSCs. Interestingly, applying the same amount of CNT to gelatin neither altered gelatin's properties notably nor augmented the effect of gelatin on cellular differentiation (not shown). Thus, the effect of CNT in the current study is mediated through the structural framework of collagen fibers. Compared to the collagen matrix, the increased fiber width, D-period and stiffness of collagen–CNT matrix facilitated the generation of extremely bipolar-shaped cells resembling neuro-epithelial progenitors (Fig. 1) [5,22]. Collagen–CNT not only led to early commitment to neural fate, but accelerated the transition to Tuj-1 as well as NeuN expressing neuronal cells (Fig. 2). Whether these cells are functionally differentiated is subject to further investigation. Since the composition of collagen and collagen–CNT matrices is essentially the same, the difference in neural differentiation is likely stemmed from the difference in their physical characteristics. This study has demonstrated the exclusive role of matrix properties on neural differentiation.

It is known that matrix cues, such as composition [19], stiffness [6] and topography [3,23], affect cell differentiation by regulating intracellular signaling pathways. With regards to neural differentiation, beta-1 integrin is highly relevant due to its specific binding to collagen type I [24]. We found while cells on collagen expressed high levels of beta-1 integrin, possibly stimulated by the highly specific interaction, cells on collagen–CNT matrix exhibited remarkable reduction in the beta-1 integrin expression level as a consequence of the augmented matrix stiffness and the altered structure (D-period, fiber thickness and possibly, ligand presentation profile). This observation indicates that cells are extremely sensitive to matrix properties and respond with dramatically different protein expression profiles, and most likely different signaling pathways. In collagen, the direct correlation between beta-1 integrin, beta-catenin and SOX1 indicates beta-1 integrin likely contributes to neural commitment on collagen matrix via beta-catenin. A possible mechanism is that beta-1 integrin stimulates integrin-linked kinase (ILK) that causes the nuclear translocation of beta-catenin [25] and induces the expression of SOX1 within the nucleus for neural commitment. On collagen–CNT matrix, however, high beta-1 integrin expression in cells is unnecessary and in fact may be detrimental to the rapid onset of SOX1 expression. An alternative mechanotransductive pathway may be involved. Recently, Du et al. observed that lower adhesion to matrix led to decreased surface expression and increased internalization of beta-1 integrin, which dictated the neural fate by a BMP/smad signaling pathway [26]. Alternatively, others have reported that the reduction in adhesion, in correspondence to the low beta-1 integrin expression, may de-activate tensional elements such as RhoA and ROCK to facilitate neural differentiation in stem cells [4,27,28]. Thus, the reduced cell adhesion strength at low beta-1 integrin expression level on the collagen–CNT matrix, associated with the increase in collagen fiber stiffness, D-period and width, likely accelerate the neural fate of hdpPSCs by triggering the intracellular mechanotransductive pathways.

The current study has demonstrated that collagen–CNT composite material is a superior matrix for hdpPSCs to induce neural cell morphology, efficient neural commitment and accelerated neural maturation. Electrophysiological studies will be conducted in order to attest the neuronal functionality. In identifying the role of beta-1 integrin, the study has laid the groundwork for more comprehensive studies on investigating neural commitment pathways on collagen and collagen–CNT and tracking beta-1 integrin expression and neural commitment dynamics on matrices of varied structural and mechanical properties.

Acknowledgment

This research was supported by NIH (R01 NS047719).

References

[1] F.M. Watt, B.L. Hogan, Out of Eden: stem cells and their niches, Sci. 287 (2000) 1427–1430.
[2] A.J. Engler, S. Sen, H.L. Sweeney, D.E. Discher, Matrix elasticity directs stem cell lineage specification, Cell 126 (2006) 677–689.
[3] M.J. Dalby, N. Gadegaard, R. Tare, A. Andar, M.O. Riehle, P. Herzyk, C.D. Wilkinson, R.O. Oreffo, The control of human mesenchymal cell differentiation using nanoscale symmetry and disorder, Nat. Mater. 6 (2007) 997–1003.
[4] E. Pacary, E. Petit, M. Bernaudin, Concomitant inhibition of prolyl hydroxylases and ROCK initiates differentiation of mesenchymal stem cells and PC12 towards the neuronal lineage, Biochem. Biophys. Res. Commun. 377 (2008) 400–406.
[5] E. Abranches, M. Silva, L. Pradier, H. Schulz, O. Hummel, D. Henrique, E. Bekman, Neural differentiation of embryonic stem cells in vitro:road map to neurogenesis in the embryo, PLoS One 4 (2009) e6286.
[6] I. Sridharan, T. Kim, R. Wang, Adapting collagen/CNT matrix in directing hESC differentiation, Biochem. Biophys. Res. Commun. 381 (2009) 508–512.
[7] Z. Strakova, M. Livak, M. Krezalek, I. Ihnatovych, Multipotent properties of myofibroblast cells derived from human placenta, Cell Tissue Res. 332 (2008) 479–488.
[8] I.N. Sneddon, The relation between load and penetration in the axisymmetric boussinesq problem for a punch of arbitrary profile, Int. J. Eng. Sci. 3 (1965) 47–57.
[9] M. Radmacher, M. Fritz, C.M. Kacher, J.P. Cleveland, P.K. Hansma, Measuring the viscoelastic properties of human platelets with the atomic force microscope, Biophys. J. 70 (1996) 556–567.
[10] J.L. Hutter, J. Chen, W.K. Wan, S. Uniyal, M. Leabu, B.M.C. Chan, Atomic force microscopy investigation of the dependence of cellular elastic moduli on glutaraldehyde fixation, J. Microsc. 219 (2005) 61–68.
[11] L. Kan, N. Israsena, Z. Zhang, M. Hu, L.R. Zhao, A. Jalali, V. Sahni, J.A. Kessler, SOX1 acts through multiple independent pathways to promote neurogenesis, Dev. Biol. 269 (2004) 580–594.
[12] S. Lowell, A. Benchoua, B. Heavey, A.G. Smith, Notch promotes neural lineage entry by pluripotent embryonic stem cells, PLoS Biol. 4 (2006) e121.
[13] D.M. Suter, D. Tirefort, S. Julien, K.H. Krause, A SOX1 to Pax6 switch drives neuroectoderm to radial glia progression during differentiation of mouse embryonic stem cells, Stem Cells 27 (2009) 49–58.
[14] U. Lendahl, L.B. Zimmerman, R.D. McKay, CNS stem cells express a new class of intermediate filament protein, Cell 60 (1990) 585–595.

[15] S.G. Wohl, C.W. Schmeer, A. Kretz, O.W. Witte, S. Isenmann, Optic nerve lesion increases cell proliferation and Nestin expression in the adult mouse eye in vivo, Exp. Neurol. 219 (2009) 175–186.

[16] M. Matsuda, R. Katoh-Semba, H. Kitani, Y. Tomooka, A possible role of the Nestin protein in the central nervous system in rat embryos, Brain Res. 723 (1996) 177–189.

[17] J.J. Otero, W. Fu, L. Kan, A.E. Cuadra, J.A. Kessler, Beta-catenin signaling is required for neural differentiation of embryonic stem cells, Development 131 (2004) 3545–3557.

[18] S. Sen, S. Kumar, Cell–matrix de-adhesion dynamics reflect contractile mechanics, Cell Mol. Bioeng. 2 (2009) 218–230.

[19] W. Ma, T. Tavakoli, E. Derby, Y. Serebryakova, M.S. Rao, M.P. Mattson, Cellextracellular matrix interactions regulate neural differentiation of embryonic stem cells, BMC Dev. Biol. 8 (2008) 90.

[20] T.I. Chao, S. Xiang, C.S. Chen, W.C. Chin, A.J. Nelson, C. Wang, J. Lu, Carbon nanotubes promote neuron differentiation from human embryonic stem cells, Biochem. Biophys. Res. Commun. 384 (2009) 426–430.

[21] Y.J. Huang, H.C. Wu, N.H. Tai, T.W. Wang, Carbon nanotube rope with electrical stimulation promotes the differentiation and maturity of neural stem cells, Small 8 (2012) 2869–2877.

[22] R. Krencik, J.P. Weick, Y. Liu, Z.J. Zhang, S.C. Zhang, Specification of transplantable astroglial subtypes from human pluripotent stem cells, Nat. Biotechnol. 29 (2011) 528–534.

[23] L.E. McNamara, R.J. McMurry, M.J. Biggs, F. Kantawong, R.O. Oreffo, M.J. Dalby, Nanotopographical control of stem cell differentiation, J. Tissue Eng. 18 (2010) 120623.

[24] Y. Xu, S. Gurusiddappa, R.L. Rich, R.T. Owens, D.R. Keene, R. Mayne, A. Höök, M.J. Höök, Multiple binding sites in collagen type I for the integrins alpha1beta1 and alpha2beta1, Biol. Chem. 275 (2000) 38981–38989.

[25] L.S. Campos, Beta1 integrins and neural stem cells: making sense of the extracellular environment, Bioessays. 27 (2005) 698–707.

[26] J. Du, X. Chen, X. Liang, G. Zhang, J. Xu, L. He, Q. Zhan, X.Q. Feng, S. Chien, C. Yang, Integrin activation and internalization on soft ECM as mechanism of induction of stem cell differentiation by ECM elasticity, Proc. Natl. Acad. Sci. 108 (2011) 9466–9471.

[27] K. Bhadriraju, M. Yang, S. Alom Ruiz, D. Pirone, J. Tan, C.S. Chen, Activation of ROCK by RhoA is regulated by cell adhesion, shape, and cytoskeletal tension, Exp. Cell Res. 313 (2007) 3616–3623.

[28] T.C. Chang, Y.C. Chen, M.H. Yang, C.H. Chen, E.W. Hsing, B.S. Ko, J.Y. Liou, K.K. Wu, Rho kinases regulate the renewal and neural differentiation of embryonic stem cells in a cell plating density-dependent manner, PLoS One 5 (2010) e9187.